

TCAQ-DM: Timestep-Channel Adaptive Quantization for Diffusion Models

Haocheng Huang^{1,2}, Jiaxin Chen^{1,2*}, Jinyang Guo³, Ruiyi Zhan^{1,2}, Yunhong Wang^{1,2}

¹State Key Laboratory of Virtual Reality Technology and Systems, Beihang University, Beijing, China

²School of Computer Science and Engineering, Beihang University, Beijing, China

³School of Artificial Intelligence, Beihang University, Beijing, China

In this document, we provide more illustration on the fluctuation of activation in distinct timesteps and channels, additional visualization on the effectiveness of the proposed TCR module, extra details and results of the effect of the proposed PAR module, as well as more quantitative results by various quantization methods on distinct datasets.

Experimental results on LSUN-Churches

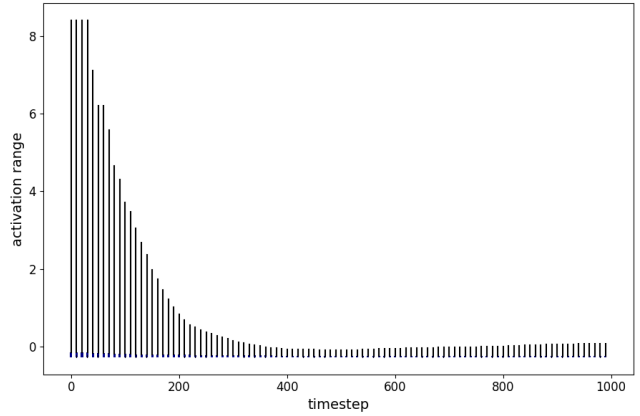
Illustration on the fluctuation of activations in distinct timesteps and channels

As described in the section of *Time-Channel Joint Reparameterization*, the activations in certain channels exhibit a narrow value range for the majority of the denoising steps, but suddenly increase in a few steps, becoming outliers, as illustrated in Fig. A. Since the averaged value is confined to a limited range, the outliers will be further amplified if the minimum value is not set as the rescale target. Conversely, if the average weight strategy is not employed, the values will not be restricted to a narrow range, leading to suboptimal performance.

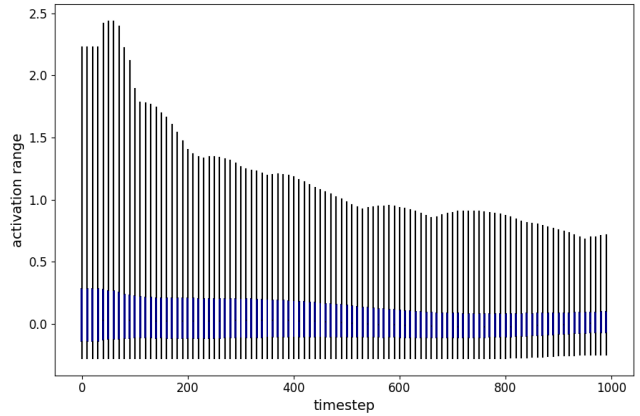
Visualization on the effectiveness of TCR

As shown in Fig. B, the activations range is restrained and balanced by our proposed TCR module, which remarkably facilitates the quantization process.

In practice, we observed that the performance of the proposed TCR degrades when the weight is quantized in low bit-widths such as the W4A8 setting. It is mainly caused by the fact that the weight is more sensitive to the change of value range than the activations in these settings, and the enlarged weights lead to more severe errors. To tackle this problem, we set a clamping range r_c to clamp the scaling vector to a narrow range. The results in Table A demonstrate that the small clamp range will benefit the final performance of TCR.



(a) Activations in distinct timesteps from the 177-th channel of **up.0.block.1.conv1**.



(b) Activations in distinct timesteps from the 91-st channel of **up.0.block.1.conv1**.

Figure A: As shown in (a), the value of some channels will suddenly rise in the final inference steps, which makes the reparameterization more challenging, while most channels are kept in a narrow range as illustrated in (b).

More details and results of PAR

The overall pipeline of the proposed progressively aligned reconstruction (PAR) is summarized in Al-

*Corresponding Author

Copyright © 2025, Association for the Advancement of Artificial Intelligence (www.aaai.org). All rights reserved.

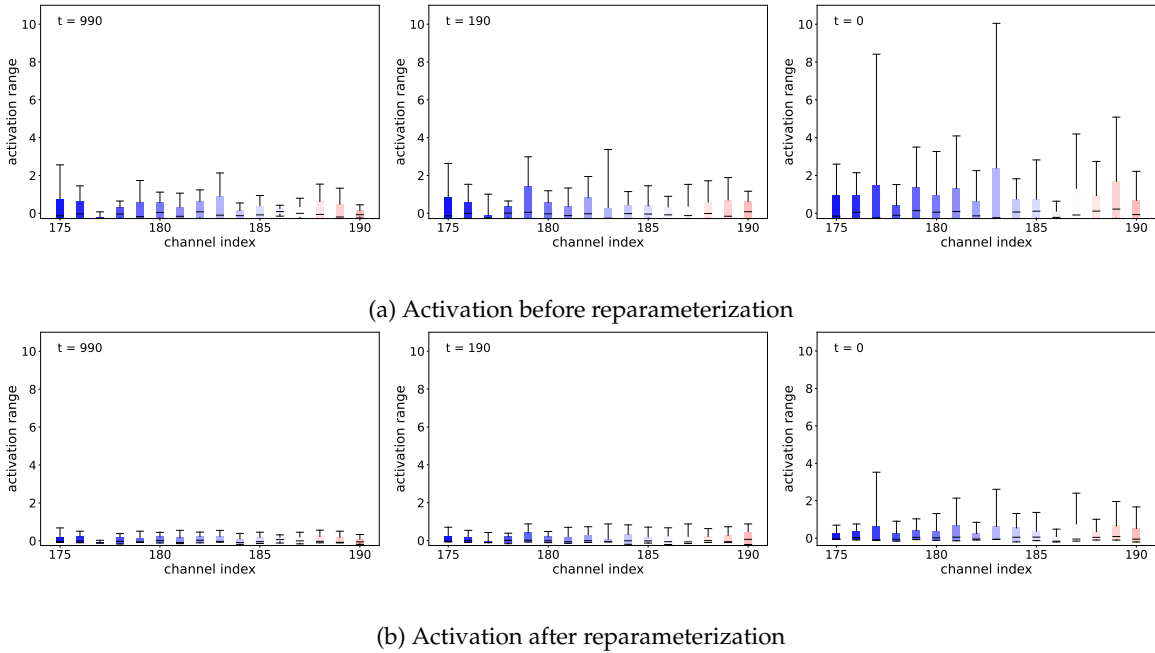


Figure B: Illustration of the effect of the reparameterization on the **up.0.block.0.conv1** layer of the DDIM model. (a) shows the activation distribution of the original model, which suffers from a severe channel variance and outliers. By comparing (a) and (b), we can observe that the fluctuated range between channels is mitigated and the value range is significantly narrowed, by adopting the proposed TCR module.

Algorithm 1: Progressively Aligned Reconstruction

Require: FP model m_f , progressive rounds p , reconstruction iterations i , Diffusion Sampler $sampler$

Ensure: Quantized model m_{qp}

- 1: $cali \leftarrow sampler(m_f)$
- 2: $m_{q_0} \leftarrow Initialization(m_f, cali)$ and basic Adaround
- 3: $n \leftarrow 0$
- 4: **while** $n < p$ **do**
- 5: $cali \leftarrow sample(m_{q_n})$
- 6: Optimize $m_{q_{n+1}}$ quantization parameters using Adaround method with calibration set $cali$ and i iterations
- 7: $n \leftarrow n + 1$
- 8: **end while**
- 9: **return** m_{qp}

Bit-width	Clamp	FID(\downarrow)	sFID(\downarrow)
W4A8	100	4.82	8.91
W4A8	50	4.76	8.95
W4A8	10	4.25	9.01
W4A8	5	4.14	9.06
W4A8	3	4.28	9.03

Table A: Ablation results of different clamp ranges on TCR on the CIFAR-10 dataset.

More Qualitative Results

In addition to Fig. 3 of the main body, we provide more qualitative results on different datasets in Fig. D to Fig. I. The experiment settings are the same as the used in the section of *Experimental Results and Analysis*. We reimplement the Q-Diffusion and TFMQ-DM methods for comparisons. As illustrated, our method generates more realistic images in most cases, showing the superiority of our method.

gorithm 1. Besides, as shown in Fig. Ca, the basic Adaround methods yield inferior performance. However, resampling the calibration set could benefit the reconstruction. We also provide more experimental results on the hyper-parameters of PAR, including the additional iteration numbers and experimental rounds. As shown in Fig. Ca (b) and (c), the proposed PAR reaches the best performance when using 10000 iterations and 2.

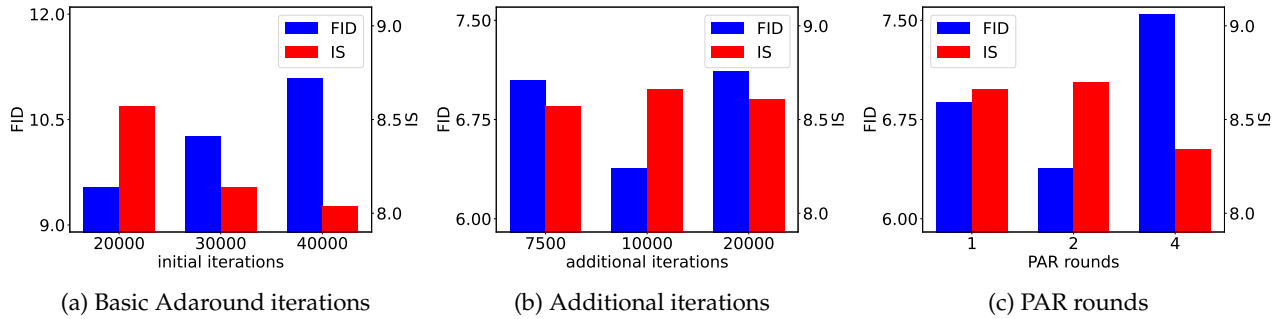


Figure C: Ablation results on PAR w.r.t. (a) the initial iterations, (b) the number of additional reconstruction iterations, and (c) the number of PAR rounds (c).

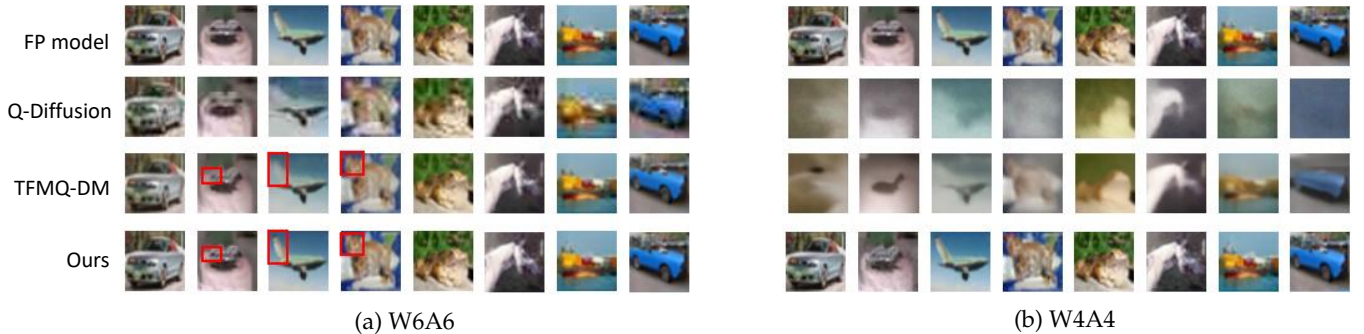
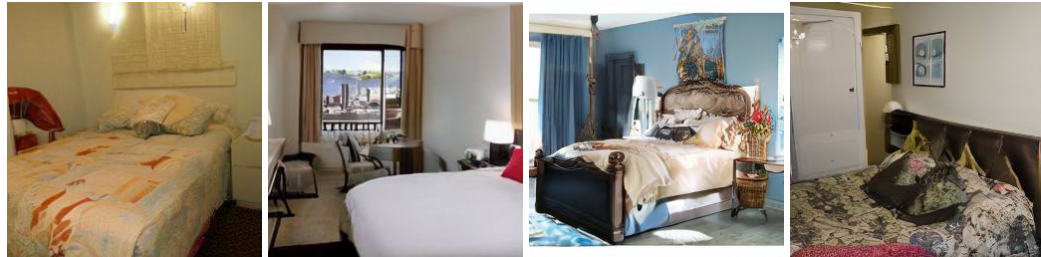


Figure D: Qualitative results on CIFAR-10 based on DDIM. The resolution of images is 32x32.



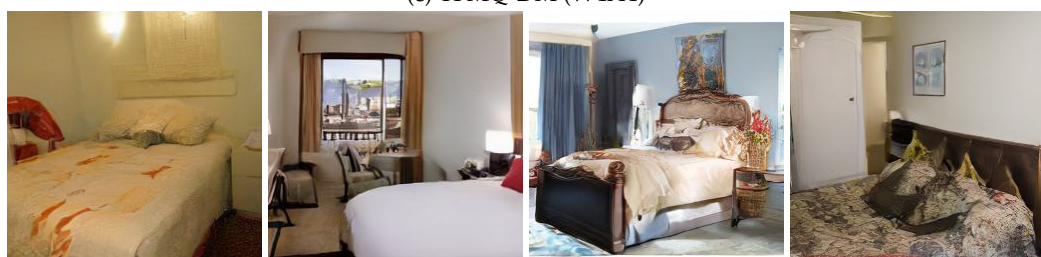
(a) Full precision model



(b) Q-Diffusion (W4A4)



(c) TFMQ-DM (W4A4)



(d) Ours (W4A4)

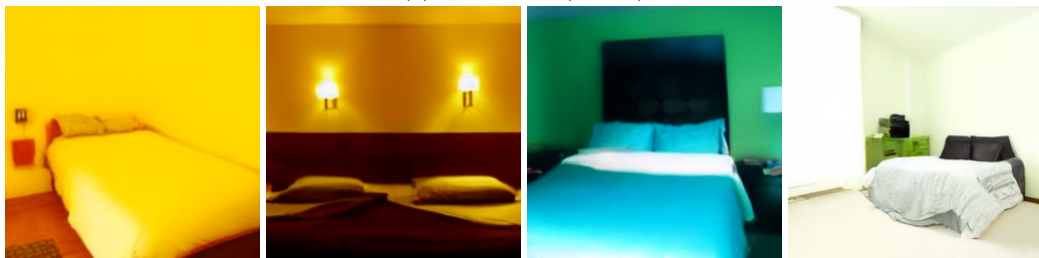
Figure E: Qualitative results on LSUN-Bedrooms based on LDM-4. The resolution of images is 256x256.



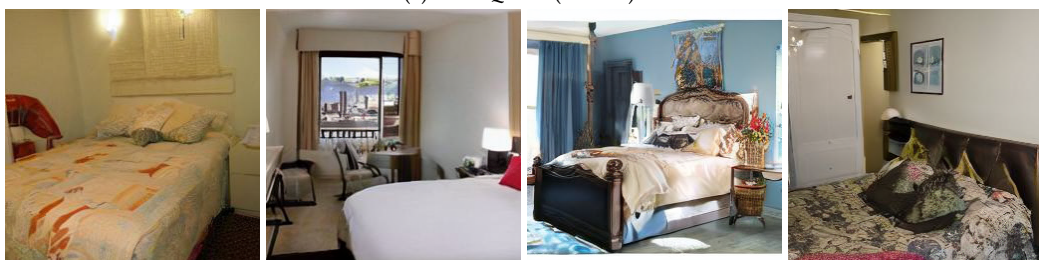
(a) FP



(b) Q-Diffusion(W4A8)



(c) TFMQ-DM(W4A8)*



(d) Ours(W4A8)

Figure F: Qualitative results on LSUN-Bedrooms based on LDM-4. The resolution of images is 256x256.



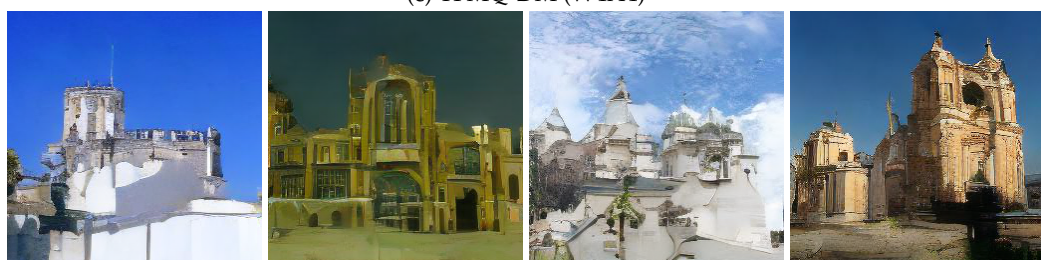
(a) Full precision model



(b) Q-Diffusion (W4A4)



(c) TFMQ-DM (W4A4)



(d) **Ours** (W4A4)

Figure G: Qualitative results on LSUN-Churches based on LDM-4. The resolution of images is 256x256.

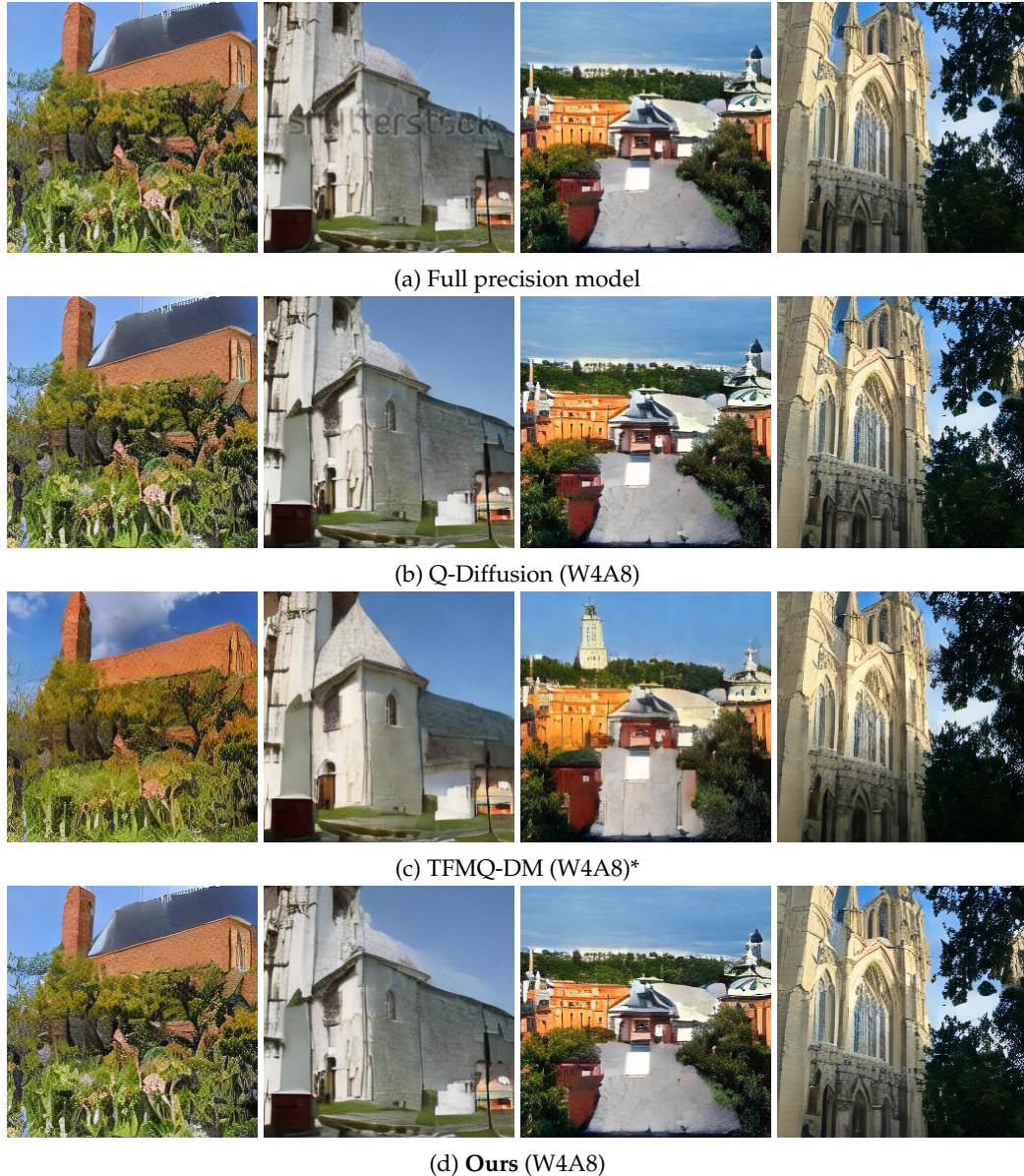


Figure H: Qualitative results on LSUN-Churches based on LDM-4. The resolution of images is 256x256.

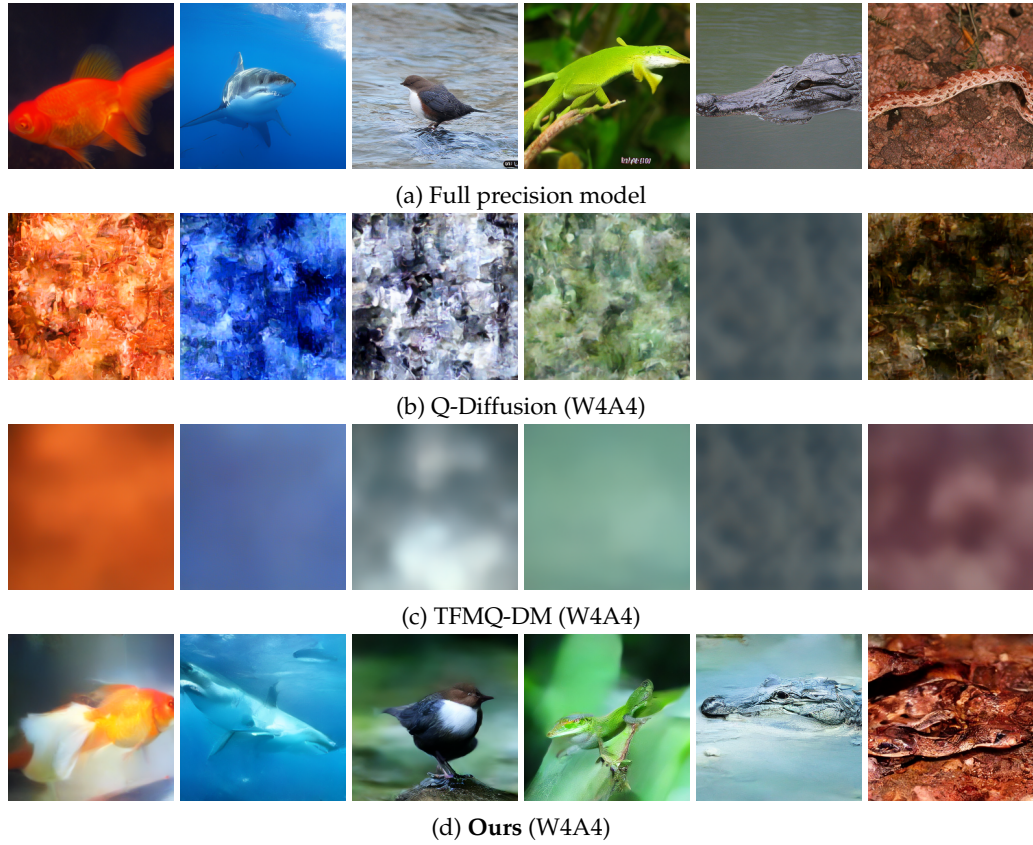


Figure I: Qualitative results on ImageNet based on LDM-4. The resolution of images is 256x256.